Journal of Photoscience (2004), Vol. 11(3), pp. 133-139

Comparative Dynamics of $tRNA^{val}$ and pBluescript II SK(+) Phagemid Studied with Ethidium Bromide and a Long-lifetime Metal-ligand Complex

Jung Sook Kang* and Ji Hye Yoon
Department of Oral Biochemistry and Molecular Biology, College of Dentistry,
Pusan National University, Busan 602-739, Korea

The metal-ligand complex, $[Ru(phen)_2(dppz)]^{2+}$ (phen=1,10-phenanthroline, dppz=dipyrido[3,2-a:2',3'-c]phenazine) (RuPD), was used as a spectroscopic probe for studying nucleic acid dynamics. The RuPD complex displays a long lifetime and a molecular light switch property upon DNA binding due to shielding of its dppz ligand from water. To show the usefulness of this luminophore (RuPD) for probing nucleic acid dynamics, we compared its intensity and anisotropy decays when intercalated into the $tRNA^{val}$ and pBluescript (pBS) II SK(+) phagemid through a comparison with ethidium bromide (EB), a conventional nucleic acid probe. We used frequency-domain fluorometry with a blue light-emitting diode (LED) as the modulated light source. The mean lifetime for the $tRNA^{val}$ ($<\tau>$ = 166.5 ns) was much shorter than that for the pBS II SK(+) phagemid ($<\tau>$ = 481.3 ns), suggesting a much more efficient shielding from water by the phagemid. Because of their size difference, the anisotropy decay data showed a much shorter rotational correlation times for the $tRNA^{val}$ (99.9 and 23.6 ns) than for the pBS II SK(+) phagemid (968.7 and 39.5 ns). These results indicate that RuPD can be useful for studying nucleic acid dynamics.

key words: long-lifetime metal-ligand complex, $tRNA^{val}$, pBluescript II SK(+), Anisotropy decay, Light-emitting diode.

INTRODUCTION

Long-lifetime metal-ligand complexes (MLCs), which display decay times ranging from 100 ns to more than 10 μs, have only recently become available [1-3] and show a number of characteristics that make them versatile biophysical probes. Because of the large Stokes' shift, the MLCs do not display significant radiative or nonradiative homo energy transfer [2, 3]. In general, the MLCs display good water solubility and high thermal, chemical and photochemical stability [2, 3]. In addition, the long lifetimes of the MLCs allow the use of gated detection, which can be employed to suppress interfering autofluorescence from biological samples and can thus provide increased sensitivity [4]. Finally, most MLCs display polarized emission, making them useful for microsecond hydrodynamics.

Barton and co-workers [5-7] reported that the dipyrido[3,2-a:2',3'-c]phenazine (dppz) complexes of ruthenium appear to be prime candidates for a spectroscopic probe for nucleic acids because of their "molecular light switch" properties for DNA. Since the luminescent enhancement upon DNA binding is $\geq 10^4$, there is essentially no background with the dppz complexes of ruthenium. There are two common dppz complexes of ruthenium, the 2,2'-bipyridine (bpy) derivative $[Ru(bpy)_2(dppz)]^{2+}$ (RuBD) and the 1,10-phenanthroline (phen) derivative $[Ru(phen)_2(dppz)]^{2+}$ (RuPD). RuPD has some advantages over RuBD because of its longer lifetime and higher quantum yield [6-9]. However, with one exception [9], all anisotropy decay measurements were performed using the bpy derivative RuBD [9-12].

To evaluate further the usefulness of RuPD for probing nucleic acid dynamics, we compared its intensity and anisotropy decays intercalated into $tRNA^{val}$ and pBluescript (PBS) II SK(+) phagemids from *E. coli* XL1-Blue MRF′ through a comparison with ethidium bromide (EB), a conventional nucleic acid probe. We used frequency-domain (FD) fluorometry with a high-intensity, blue light-emitting diode (LED) as the modulated light source. With this LED we were able to directly modulate the excitation light up to 100 MHz without the need for an external modulator like a Pockels cell and to obtain very reliable time-resolved intensity and anisotropy decays with simpler and low cost instrumentation.

MATERIALS AND METHODS

Materials

LB-medium from Beckton, Dickinson and Company (Franklin Lakes, USA); $tRNA^{val}$, agarose and ampicillin from Sigma (St. Louis, USA); pBS II SK(+) phagemid (2961 bp) and *E. coli* XL1-Blue MRF′ from Stratagene (La Jolla, USA); and plasmid mega kit from Qiagen Inc. (Valencia, USA). $tRNA^{val}$ was used without further purification, and RuPD was synthesized by the method described previously [12]. All

*To whom correspondence should be addressed.
E-mail: jsokang@pusan.ac.kr
Received December 8, 2004; Accepted December 28, 2004

other chemicals were of the reagent grade, and water was deionized with a Milli-Q system. All measurements were carried out in REACT4 buffer.

Absorption and steady-state fluorescence measurements

pBS II SK(+) phagemids were purified with Qiagen plasmid mega kit from 500 ml overnight cultures of *E. coli* XL1-Blue MRF′ in LB-medium containing ampicillin. About 5-10 mM stock solution of RuPD was prepared in dimethylformamide. The $tRNA^{val}$ concentration was 1 mM nucleotide while that of phagemid was 300 μM bp. The concentrations of $tRNA^{val}$ and DNA were determined using molar extinction coefficients of 8,200 $M^{-1}cm^{-1}$ (expressed as nucleotide) and 13,000 $M^{-1}cm^{-1}$ (expressed as bp) at 260 nm, respectively. The concentrations of EB and RuPD were 5 and 15 μM, respectively, and were determined using molar extinction coefficients of 5,200 M^{-1} cm^{-1} at 518 nm and 21,000 $M^{-1}cm^{-1}$ at 440 nm, respectively. UV-visible absorption spectra were measured with a Hewlett-Packard 8453 diode array spectrophotometer. Steady-state intensity and anisotropy measurements were carried out using a Cary Eclipse fluorescence spectrophotometer (Varian Inc., Palo Alto, USA).

The intensity of the components of the fluorescence that were parallel (I_w) and perpendicular (I_{VH}) to the direction of the vertically polarized excitation light was determined by measuring the emitted light through polarizers oriented vertically and horizontally. The steady-state anisotropy is given by:

$$r = \frac{I_{VV} - GI_{VH}}{I_W + 2GI_{VH}} \tag{1}$$

where G is a grating correction factor for the monochromator's transmission efficiency for vertically and horizontally polarized light. This value is given by the ratio of the fluorescence intensities of the vertical (I_{HV}) to horizontal (I_{HH}) components when the exciting light is polarized in the horizontal direction.

FD intensity and anisotropy decay measurements

Measurements were performed with an ISS Koala instrument (ISS Inc., Champaign, USA) using a blue LED LNG992CFBW (Panasonic, Japan) as the excitation source. An LED driver LDX-3412 (ILX Lightwave, Boseman, USA) provided 30 mA of current at frequencies from 0.07 to 100 MHz. A 480 ± 20 nm interference filter and a 630 nm cut-off filter were used for isolating excitation and emission, respectively. Rhodamine B in water (τ = 1.68 ns) was utilized as a lifetime standard. All measurements were performed at 25°C.

The intensity decays were recovered from the FD data in terms of a multiexponential model using nonlinear least squares analysis [13, 14]:

$$I(t) = \sum_{i=1}^{n} \alpha_i e^{-t/\tau_i} \tag{2}$$

where the preexponential factor α_i is the amplitude of each component, $\Sigma\alpha_i$=1.0, τ_i is the decay time, and n is the number of exponential components. Mean lifetimes were calculated by:

$$\langle \tau \rangle = \frac{\sum_i \alpha_i \tau_i^2}{\sum_i \alpha_i \tau_i} = \sum_i f_i \tau_i \tag{3}$$

where f_i is the fractional steady-state contribution of each component to the total emission, and Σf_i is normalized to unity. f_i is given by:

$$f_i = \frac{\alpha_i \tau_i}{\sum_j \alpha_j \tau_j} \tag{4}$$

The calculated (c) values of the phase $\phi_{c\omega}$ and modulation $m_{c\omega}$ at each modulation frequency ω are given by:

$$\phi_{c\omega} = \arctan(N_\omega / D_\omega) \tag{5}$$

$$m_{c\omega} = (N_\omega^2 + D_\omega^2)^{1/2} \tag{6}$$

where

$$N_\omega = \sum_i \frac{\alpha_i \omega \tau_i^2}{1 + \omega^2 \tau_i^2} / \sum_i \alpha_i \tau_i \tag{7}$$

$$D_\omega = \sum_i \frac{\alpha_i \tau_i}{1 + \omega^2 \tau_i^2} / \sum_i \alpha_i \tau_i \tag{8}$$

The values of α_i and τ_i were determined by minimizing χ_R^2 values:

$$\chi_R^2 = \frac{1}{\nu} \sum_\omega \left[\left(\frac{\phi_\omega - \phi_{c\omega}}{\delta\phi} \right)^2 + \left(\frac{m_\omega - m_{c\omega}}{\delta m} \right)^2 \right] \tag{9}$$

where ν is the number of degrees of freedom, and ϕ_ω and m_ω are the measured phase and modulation, respectively. $\delta\phi$ and δm are the experimental uncertainties in the measured phase and modulation values and were set at 0.2° and 0.005, respectively.

The FD anisotropy decays were also analyzed in terms of the multiexponential model using nonlinear least squares analysis [15, 16]:

$$r(t) = \sum_i r_0 g_i e^{-t/\theta_i} \tag{10}$$

where g_i is the amplitude of the anisotropy component with a rotational correlation time θ_i, Σg_i = 1.0, and r_0 is the anisotropy in the absence of rotational diffusion. The total anisotropy r_0 was a fitted parameter.

The phase shift (Δ_ω) at the modulation frequency ω is given by

$$\Delta_\omega = \phi_{VH} - \phi_{VV} \tag{11}$$

where ϕ_{VH} and ϕ_{VV} are the perpendicular (VH) and parallel (VV) components of the emission. The modulation ratio Λ_ω is

$$\Lambda_\omega = m_{VV}/m_{VH} \tag{12}$$

where m_{VV} and m_{VH} are the amplitudes of the parallel (*VV*) and the perpendicular (*VH*) components of the modulated emission, respectively. The modulated anisotropy r_ω was calculated by:

$$r_\omega = \frac{\Lambda_\omega - 2}{\Lambda_\omega + 2} \tag{13}$$

The calculated values of Δ_ω and Λ_ω are given by

$$\Delta_{c\omega} = \arctan\left(\frac{D_{VV}N_{VH} - N_{VV}D_{VH}}{N_{VV}N_{VH} + D_{VV}D_{VV}}\right) \tag{14}$$

$$\Lambda_{c\omega} = \left(\frac{N_{VV}^2 + D_{VV}^2}{N_{VH}^2 + D_{VH}^2}\right)^{1/2} \tag{15}$$

where

$$N_k = \int_0^\infty I_k(t)\sin \omega t dt \tag{16}$$

$$D_k = \int_0^\infty I_k(t)\cos \omega t dt \tag{17}$$

In this expression the subscript k indicates the orientation, parallel (*VV*) or perpendicular (*VH*). The parameters describing the anisotropy decay are obtained by minimizing χ_R^2 values:

$$\chi_R^2 = \frac{1}{\nu}\sum_\omega\left[\left(\frac{\Delta_\omega - \Delta_{c\omega}}{\delta\Delta}\right)^2 + \left(\frac{\Lambda_\omega - \Lambda_{c\omega}}{\delta\Lambda}\right)^2\right] \tag{18}$$

where $\delta\Delta$ and $\delta\Lambda$ are the experimental uncertainties in the differential phase and modulation ratio values and were set at 0.2° and 0.005, respectively.

RESULTS AND DISCUSSION

Fig. 1 shows the chemical structures of EB and RuPD. The emission spectra of EB and RuPD intercalated into the tRNA^{val} and pBS II SK(+) phagemid are shown in Fig. 2. Both probes showed blue-shifted emission when intercalated into tRNA^{val}. EB and RuPD showed emission peaks at about 600 and 620 nm, respectively. As expected, we observed much lower steady-state anisotropy values with RuPD than EB because of its longer lifetime (Fig. 3). For both probes tRNA^{val} showed much lower steady-state anisotropy values at all temperatures due to its small size (Fig. 3). The steady-state anisotropy values of RuPD when intercalated into the pBS II SK(+) phagemid (2961 bp) were lower than in our previous studies using RuBD intercalated into the pTZ18U plasmid (2860 bp) [10,11]. Because the size difference between pBS II SK(+) and pTZ18U is small, this is mainly due to longer lifetime of RuPD. Importantly, although RuPD showed lower steady-state anisotropy values, it clearly showed the size difference between tRNA^{val} and pBS II SK(+) phagemid.

The FD intensity decays of EB and RuPD intercalated into

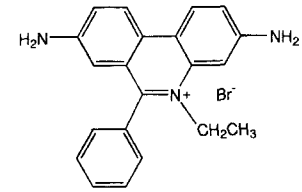

EB

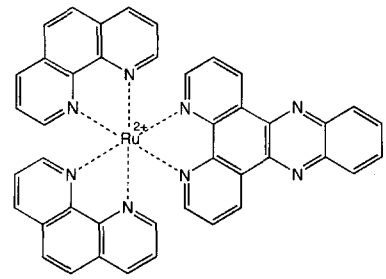

RuPD

Figure 1. Chemical structures of ethidium bromide (EB) and $[Ru(phen)_2(dppz)]^{2+}$ (RuPD).

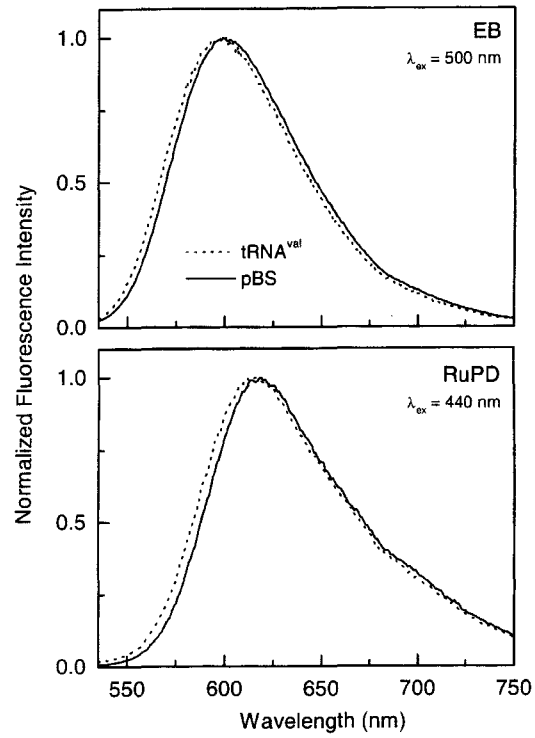

Figure 2. Emission spectra of EB (top) and RuPD (bottom) intercalated into tRNA^{val} and pBluescript II SK(+) phagemid (pBS).

the tRNA^{val} and pBS II SK(+) phagemid are shown in Fig. 4. For EB, the best fits of the intensity decays were obtained using the two exponential model. The intensity decays of RuPD were best fit by a triple exponential decay. Table 1 shows the intensity decay results for EB and RuPD intercalated into the tRNA^{val} and pBS II SK(+) phagemid. In

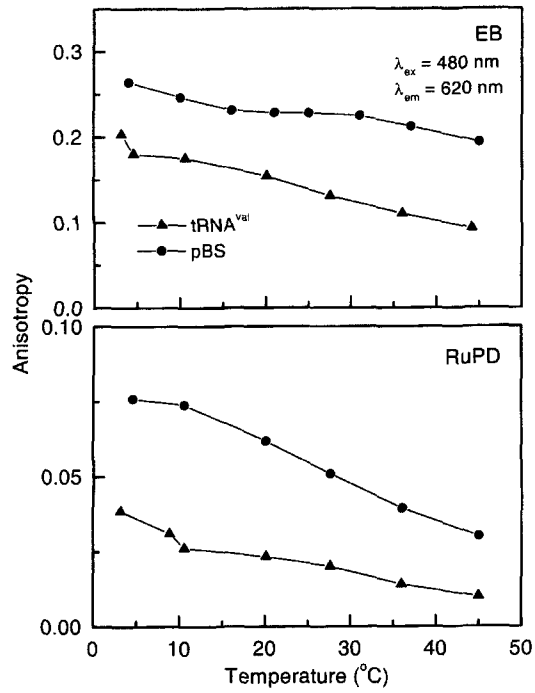

Figure 3. Temperature-dependent steady-state anisotropy of EB (top) and RuPD (bottom) intercalated into tRNA^{val} and pBluescript II SK(+) phagemid (pBS). The steady-state anisotropy values were calculated by Eq. (1).

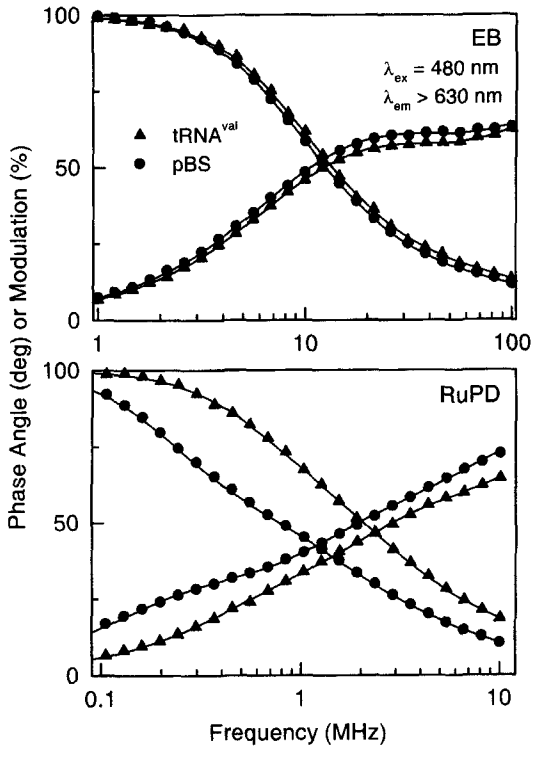

Figure 4. Intensity decays of EB (top) and RuPD (bottom) intercalated into tRNA^{val} and pBluescript II SK(+) phagemid (pBS). The symbols represent the measured phase and modulation values. The solid lines show the best multiexponential fits to the data.

Table 1. Multiexponential intensity decay analyses of ethidium bromide (EB) and $[Ru(phen)_2(dppz)]^{2+}$ (RuPD) intercalated into tRNA^{val} and pBluescript II SK(+) phagemid (PBS)

Probe	Nucleic acid	τ_i (ns)	α_i	f_i[a]	$\langle\tau\rangle$[a] (ns)	χ_R^2[b]
EB	tRNA^{val}	21.3	0.37	0.89	19.3	1.2
		1.5	0.63	0.11		
	PBS	22.6	0.41	0.92	20.9	1.3
		1.4	0.59	0.08		
RuPD	tRNA^{val}	289.3	0.11	0.45	166.5	2.0
		76.8	0.38	0.44		
		14.6	0.51	0.11		
	PBS	808.0	0.09	0.54	481.3	2.8
		121.2	0.40	0.35		
		29.5	0.51	0.11		

[a]Fractional intensities f_i and mean lifetimes $\langle\tau\rangle$ were calculated using Eqs. (4) and (3), respectively.

[b]The χ_R^2 values were calculated by Eq. (9), and the standard errors of phase angle and modulation were set at 0.2° and 0.005, respectively.

the case of EB, the mean lifetime values for the tRNA^{val} and pBS II SK(+) phagemid were 19.3 and 20.9 ns, respectively. However, we observed much shorter mean lifetime for tRNA^{val} than that for the pBS II SK(+) phagemid using RuPD. The mean lifetime values for the tRNA^{val} and pBS II SK(+) phagemid measured with RuPD were 166.5 and 481.3 ns, respectively (Table 1). This result suggests that the RuPD MLC was much more efficiently shielded from water in the phagemid than in the tRNA^{val}, resulting in a longer lifetime. Thus, it seems that the pBS II SK(+) phagemid adopts much more favorable conformations for RuPD intercalation than tRNA^{val}. The lifetime value of RuPD intercalated into the pBS II SK(+) phagemid (Table 1) is larger than reported previously [6-9, 17]. The earlier values ranging from 170 ns to 380 ns were mostly measured by time-correlated single photon counting [6, 7, 9, 17], which weights the shorter decay times more heavily than does the FD measurements. In addition, resolution of a triple exponential decay is difficult [18], and the individual decay times are subject to significant uncertainty.

In addition to the intensity decay measurements, we also measured the anisotropy decays of EB and RuPD intercalated into the tRNA^{val} and pBS II SK(+) phagemid (Fig. 5 and 6), and the results are summarized in Table 2. For both probes, the best fits of the anisotropy decay data were obtained using the two correlation time model. In the case of EB intercalated into tRNA^{val}, the slow rotational correlation time (25.6 ns) appears to be consistent with that expected for overall rotational mobility of tRNA^{val}. The value is comparable to the values reported previously for tRNA^{val} by fluorescence anisotropy decays [19] and by electrooptical measurements [20]. The fast rotational correlation time (9.8 ns) may be due to independent motion of two helical arms of the L-shaped structure of tRNA^{val} [21]. For RuPD, the slow and fast rotational correlation times were 99.9 and 23.6 ns, respectively,

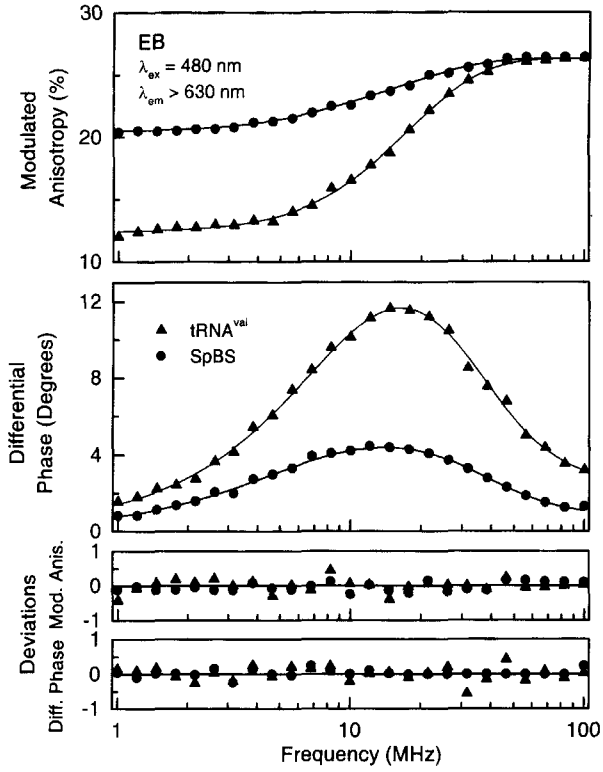

Fig. 5. Anisotropy decays of EB intercalated into tRNA^{val} and pBluescript II SK(+) phagemid (pBS). The symbols in the first and second panels represent the modulated anisotropy and the measured phase shift values, respectively. The modulated anisotropy values were calculated from measured Λ_ω using Eq. (13). The solid lines show the best multiexponential fits to the data. The lower two panels show plots of the residuals between the experimental data and the fitted curve.

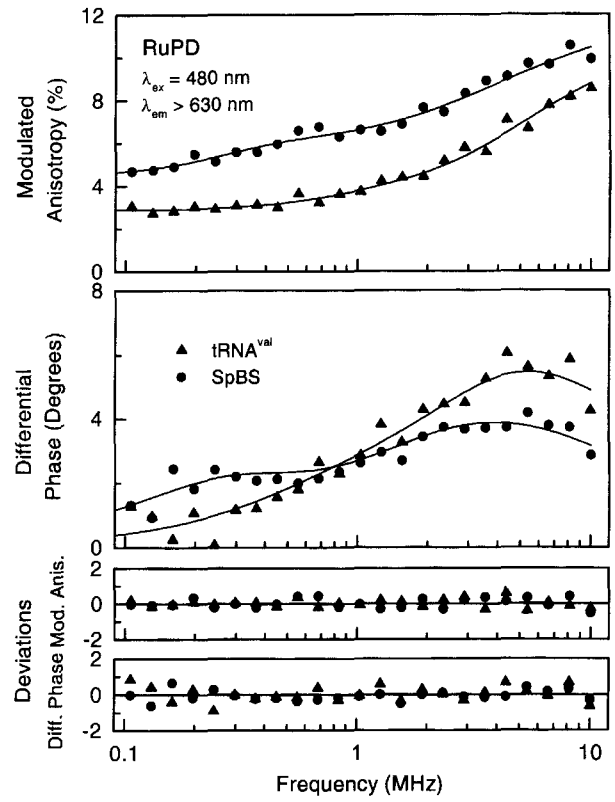

Fig. 6. Anisotropy decays of RuPD intercalated into tRNA^{val} and pBluescript II SK(+) phagemid (pBS). All conditions are the same as in Fig. 5.

when intercalated into tRNA^{val} (Table 2). The fast rotational correlation time (23.6 ns) is comparable to the slow rotational correlation time using EB (25.6 ns). Thus, it seems that the fast rotational correlation time of RuPD is consistent with the overall rotational mobility of tRNA^{val}. However, at present, we are not able to interpret the slow rotational correlation time of RuPD (99.9 ns). It may imply the presence of aggregates of the tRNA^{val}-RuPD complex. We used somewhat high concentrations of both tRNA^{val} (1 mM nucleotide) and RuPD (15 μM). In addition, the probe to tRNA^{val} molar ratio, about 1:1, may be high. Further experimentation is required to clarify this. For the pBS II SK(+) phagemid, the slow and fast rotational correlation times appear to be consistent with the bending (flexure of the helix axis) and torsional (twisting of bp) motions of phagemids, respectively, for both probes. The torsional motion of DNA occurs in 1-100 ns, while the bending motion of DNA ranges from about 100 ns to more than 100 μs (22). Information on the rotational motion is usually available over a time scale not exceeding three times the lifetime of the fluorophore, after which there is too little signal for accurate anisotropy measurements. So, the slow rotational correlation time (153.9 ns) of the phagemid measured with EB ($<\tau>$ = 20.9 ns) does not seem to be very reliable. Fig. 5 and 6 (first panels) show the modulated anisotropy values for EB and RuPD intercalated into the tRNA^{val} and pBS II SK(+) phagemid. We observed much lower modulated anisotropy values using RuPD than EB, which is in agreement with the results of our steady-state anisotropy measurements. For both probes tRNA^{val} showed lower modulated anisotropy values, which also coincides with our steady-state anisotropy results (Fig. 5 and 6).

In this study, we demonstrated the usefulness of RuPD, a long-lifetime MLC for probing the comparative dynamics of the tRNA^{val} and pBS II SK(+) phagemid through a comparison with EB, a conventional DNA probe. The results of both steady-state anisotropy measurements and time-resolved anisotropy decay measurements clearly showed that RuPD can be useful for studying hydrodynamics of DNA and small nucleic acid such as tRNA^{val}. Importantly, the use of RuPD, which has a lifetime of about 480 ns (Table 1), enabled us to extend the measurable time scale of DNA dynamics to microsecond. We could measure the rotational correlation time about 1 μs (Table 2). However, as in our previous studies (10,11), it has to be pointed out that the lifetime of RuPD is still short to measure the slower bending motions or end-over-end tumbling motions of the plasmids.

The use of long-lifetime MLCs to measure DNA dynamics

Table 2. Multiexponential anisotropy decay analyses of ethidium bromide (EB) and $[Ru(phen)_2(dppz)]^{2+}$ (RuPD) intercalated into $tRNA^{val}$ and pBluescript II SK(+) phagemid (PBS)

Probe	Nucleic Acid	θ_i (ns)	$r_0*g(i)$	$\Sigma(r_0*g(i))$	$\chi_i^{2a)}$
EB	$tRNA^{val}$	25.6	0.105	0.272	1.9
		9.8	0.167		
	PBS	153.9	0.211	0.265	4.2
		9.4	0.054		
RuPD	$tRNA^{val}$	99.9	0.022	0.114	3.7
		23.6	0.092		
	PBS	968.7	0.044	0.117	3.3
		39.5	0.073		

[a)]The χ_i values were calculated by Eq. (18), and the standard errors of phase angle and modulation were set at 0.2° and 0.005, respectively.

is just beginning [2, 3, 9-12]. Barton and coworkers [6] showed that RuBD exhibited sensitivity to conformational differences in DNA because of the incomplete shielding of the dppz ligand from water in the presence of bpy in contrast to the other phen derivative RuPD. However, the phen derivative RuPD has some advantages over the other bpy derivative RuBD. The lifetimes of RuBD bound to DNA are about 100-150 ns [6, 7, 9-12, 23]. RuPD showed still longer lifetimes bound to DNA, with a mean decay time near 480 ns (Table 1). Besides, the quantum yield of RuPD (Q=0.017) [8] is more than twice that of RuBD (Q=0.008) [23]. Because of longer lifetime and higher quantum yield than the bpy derivative, RuPD is expected to have numerous applications in studies of nucleic acid structure and dynamics.

An important point of the present study is our use of a semiconductor light source for the FD intensity and anisotropy decay measurements. A variety of LEDs including the high intensity UV, blue and green LEDs have been developed as an inexpensive and convenient light source. LEDs are easily modulated up to hundreds of MHz without the need for a Pockels cell [24]. We believe that LEDs will become an ideal light source for measuring microsecond dynamics of biological macromolecules.

Acknowledgments

This research was supported by Medical Research Institute Grant (2002-11), Pusan National University. JSK thanks Professor Joseph R. Lakowicz, Center for Fluorescence Spectroscopy, Baltimore, USA for the gift of RuPD. JSK is also grateful to Professor Govind Rao, Dept. of Chemical and Biochemical Engineering, The University of Maryland, Baltimore County, Baltimore, USA for providing instrumentation.

REFERENCES

1. DeGraff, B. A. and Demas, J. N. (1994) Direct measurement of rotational correlation times of luminescent ruthenium(II) molecular probes by differential polarized phase fluorometry. *J. Phys. Chem.* **98**, 12478-12480.
2. Lakowicz, J. R., Gryczinski, I., Piszczek, G., Tolosa, L., Nair, R., Johnson, M. L. and Nowaczyk, K. (2000) Microsecond dynamics of biological molecules. *Methods Enzymol.* **323**, 473-509.
3. Terpetschnig, E., Szmacinski, H. and Lakowicz, J. R. (1997) Long-lifetime metal-ligand complexes as probes in biophysics and clinical chemistry. *Methods Enzymol.* **278**, 295-321.
4. Haugen, G. R. and Lytle, F. E. (1981) Quantitation of fluorophores in solution by pulsed laser excitation of time-filtered detection. *Anal. Chem.* **53**, 1554-1559.
5. Friedman, A. E., Chambron, J. -C., Sauvage, J. -P., Turro, N. J. and Barton, J. K. (1990) Molecular "light switch" for DNA: $Ru(bpy)_2(dppz)^{2+}$. *J. Am. Chem. Soc.* **112**, 4960-4962.
6. Jenkin, Y., Friedman, A. E., Turro, N. J. and Barton, J. K. (1992) Characterization of dipyridophenazine complexes of ruthenium(II): The light switch effect as a function of nucleic acid sequence and conformation. *Biochemistry* **31**, 10809-10816.
7. Murphy, C. J. and Barton, J. K. (1993) Ruthenium complexes as luminescent reporters of DNA. *Methods Enzymol.* **226**, 576-594.
8. Kang, J. S. and Lakowicz, J. R. (2001) Fluorescence resonance energy transfer in calf thymus DNA from a long-lifetime metal-ligand complex to nile blue. *J. Biochem. Mol. Biol.* **34**, 551-558.
9. Malak, H., Gryczinski, I., Lakowicz, J. R., Meyers, G. J. and Castellano, F. N. (1997) Long-lifetime metal-ligand complexes as luminescent probes for DNA. *J. Fluorescence* **7**, 107-112.
10. Kang, J. S., Abugo, O. O. and Lakowicz, J. R. (2002) Dynamics of supercoiled and linear pTZ18U plasmids observed with a long-lifetime metal-ligand complex. *Biopolymers* 67, 121-128.
11. Kang, J. S., Abugo, O. O. and Lakowicz, J. R. (2002) Dynamics of supercoiled and relaxed pTZ18U plasmids probed with a long-lifetime metal-ligand complex. *J. Biochem. Mol. Biol.* **35**, 389-394.
12. Lakowicz, J. R., Malak, H., Gryczynski, I., Castellano, F. N. and Meyer, G. J. (1995) DNA dynamics observed with long lifetime metal-ligand complexes. *Biospectroscopy* **1**, 163-168.
13. Gratton, E., Limkeman, M., Lakowicz, J. R., Maliwal, B. P., Cherek, H. and Laczko, G. (1984) Resolution of mixtures of fluorophores using variable-frequency phase and modulation data. *Biophys. J.* **46**, 479-486.
14. Lakowicz, J. R., Laczko, G., Cherek, H., Gratton, E. and Limkeman, M. (1984) Analysis of fluorescence decay kinetics from variable-frequency phase-shift and modulation data. *Biophys. J.* **46**, 463-477.
15. Lakowicz, J. R. and Gryczinski, I. (1991) Frequency-domain fluorescence spectroscopy; in *Topics in Fluorescence Spectroscopy, Volume 1, Techniques*, Lakowicz, J. R. (ed.), pp. 293-355, Plenum Press, New York, USA.
16. Lakowicz, J. R., Cherek, H., Kusba, J., Gryczinski, I. and Johnson, M. L. (1993) Review of fluorescence anisotropy

decay analysis by frequency-domain fluorescence spectroscopy. *J. Fluorescence*, **3**, 103-116.

17. Holmin, R. E., Stemp, E. D. A. and Barton, J. K. (1998) $Ru(phen)_2dppz^+$ luminescence: dependence on DNA sequences and groove-binding agents. *Inorg. Chem.*, **37**, 29-34.
18. Lakowicz, J. R. (1999) *Principles of Fluorescence Spectroscopy*, 2nd ed., pp. 98-101, Kluwer Academic/Plenum Publishers, New York, USA.
19. Thomas, J. C., Schurr, J. M. and Hare, D. R. (1984) Rotational dynamics of transfer ribonucleic acid: effect of ionic strength and concentration. *Biochemistry* **23**, 5407-5413.
20. Porschke, D. and Antosiewicz, J. (1990) Permanent dipole moment of tRNA's and variation of their structure in solution. *Biophys. J.* **58**, 403-411.
21. Kang, J. S. (2000) Dynamics of $tRNA^{val}$ measured with a long-lifetime metal-ligand complex. *J. Photoscience* **7**, 155-159.
22. Schurr, J. M., Fujimoto, B. S., Wu, P. and Song, L. (1992) Fluorescence studies of nucleic acids: dynamics, rigidities, and structures; in *Topics in Fluorescence Spectroscopy, Volume 3, Biochemical Applications*, Lakowicz, J. R. (ed.), pp. 137-229, Plenum Press, New York, USA.
23. Lakowicz, J. R., Piszczek, G. and Kang, J. S. (2001) On the possibility of long-wavelength long-lifetime high-quantum yield luminophores. *Anal. Biochem.* **288**, 62-75.
24. Sipior, J., Carter, J. M., Lakowicz, J. R. and Rao, G. (1996) Single quantum well light-emitting diodes demonstrated as excitation sources for nanosecond phase modulation fluorescence lifetime measurements. *Rev. Sci. Instr.* **67**, 3795-3798.